EXPERIMENTAL CONFIRMATION OF DEEP NULLING

E. Serabyn

Jet Propulsion Laboratory, Mail Stop 171-113, 4800 Oak Grove Drive
California Institute of Technology, Pasadena, CA 91109, USA

ABSTRACT

Nulling interferometry has great potential in the search for planetary companions and exozodiacal disks, but the various approaches proposed remain largely unproven. Here laboratory confirmation of deep nulling is reported. Using a fiber-coupled rotational shearing interferometer, a red laser diode has been nulled to a part in several hundred thousand, and the laser null has been stabilized to a part in 10,000. Single-polarization white light of 10% bandwidth has also been nulled to a part in 10,000.

Key words: nulling interferometry; rotational shearing interferometer.

1. INTRODUCTION

The direct detection of radiation from planets beyond our solar system has thus far been prevented by the small angular separation and high brightness contrast characteristic of star-planet systems. If our solar system were viewed from a distance of 10 pc, the radius of the Earth's orbit would subtend a mere $0.1''$, while the Sun/Earth contrast ratio at visual wavelengths would exceed 10^9:1. However, while orbital radii are fixed constraints, contrast ratios are amenable to modification in at least two ways: shifting the observational wavelength into the infrared, where planetary thermal emission spectra peak, and using an optical approach which is capable of selectively dimming the star relative to its surroundings. In the latter regard, "nulling" interferometry has great promise (Shao & Colavita 1992, Leger *et al.* 1996, Woolf & Angel 1998, Beichman, Woolf & Lindensmith 1999), but remains largely unproven. In the following, an overview of nulling with a fiber-coupled rotational shearing interferometer is given, and recent experimental results confirming the viability of this approach are summarized.

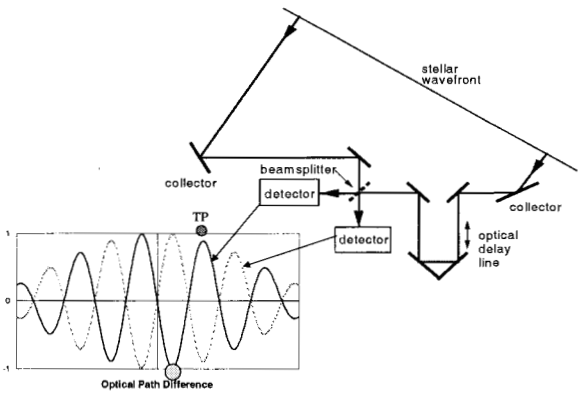

Figure 1. Schematic diagram of a standard stellar interferometer and the fringe patterns at the two outputs. Conceptually the goal of nulling is to place the star at the bottom of a deep destructive fringe (e.g., just right of center), and an accompanying terrestrial planet (TP) near the top of a constructive fringe.

2. NULLING BASICS

The basic premise of nulling interferometry is quite simple: interferometrically combine the starlight incident on a pair of telescopes in such a way that at zero optical path difference (OPD) between the beams, the two electric field vectors arrive with a relative inversion, enabling near-perfect starlight subtraction. In other words, the goal is to place a deep destructive interference fringe across the star (Bracewell 1978), while at the same time allowing emission from off-axis sources to be transmitted through neighboring constructive interference fringes (Fig. 1). Thus even though the star is nulled to a deep level, appropriately situated off-axis planets are not greatly attenuated. The challenge then is to devise a realistic optical system which can simultaneously null a star to deep levels in both polarizations and at all wavelengths across the passband of interest.

For the nulling approach to be effective, the stellar cancellation must be very deep, with residual light levels on the order of a part in 10^6 for terrestrial

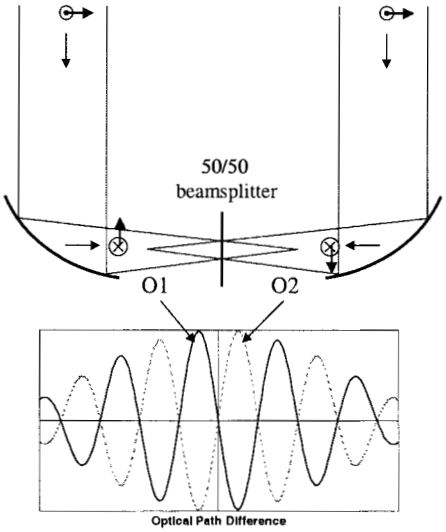

Figure 2. Original nulling scheme described by Bracewell & MacPhie (1979).

planet detection, and a part in 10^{3-4} for detection of faint exozodiacal disks (Traub, Carleton & Angel 1996, Angel 1998, Beichman, Woolf & Lindensmith 1999, Serabyn, Colavita & Beichman 2000). Of course, the given null depths refer to the net nulls integrated across the passband. Such deep achromatic nulling cannot possibly be provided by a standard stellar interferometer, because as Figures 1 and 2 show, the inherent symmetry of such systems implies that at zero OPD, the two beamsplitter outputs are equivalent, with each receiving half the incident power. To effect deep cancellation, a finite OPD must therefore be introduced. An offset of a quarter of the average wavelength will optimize the cancellation in this case (Figs. 1 & 2), but since a quarter wavelength is clearly a chromatic quantity, it is evident that all wavelengths cannot cancel simultaneously for a non-zero OPD setting. Indeed, this is the reason why the original nulling scheme (Fig. 2) of Bracewell & MacPhie (1979) fails to provide a very deep null. (Of course, there is an even more serious problem with the scheme of Fig. 2, in that the fringes in the two polarization states actually cancel each other completely in such a perfectly symmetric system).

A more achromatic method of inducing destructive interference is therefore necessary, the ideal case being completely wavelength independent cancellation at zero OPD. What is thus desired is a set of fringes complementary to those present at the output of a standard laboratory Michelson interferometer (Fig. 3), for which an achromatic *constructive* fringe occurs at zero OPD. An ideal achromatic destructive fringe (solid curve in Fig. 3) can indeed be generated by subtracting, instead of adding, the two incident electric fields. In fact, conservation of energy implies that such subtraction must apply at the complementary output of a laboratory Michelson interferometer. However, as this output rejects the light back

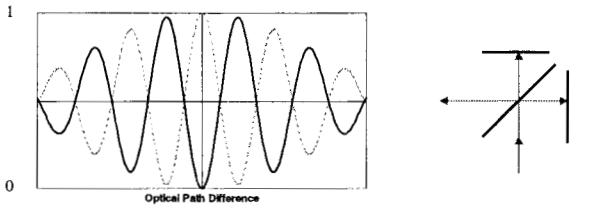

Figure 3. Standard laboratory Michelson interferometer, and the associated fringe pattern (dotted line) at the output port. For deep achromatic nulling, inverting the fringes (solid line) would be desirable, so that achromatic cancellation occurs at zero OPD.

into the input port, it is not readily accessible, and so another route must be sought.

3. NULLING WITH A ROTATIONAL SHEARING INTERFEROMETER

One approach to electric field subtraction is to introduce a relative flip between the two fields to be combined. Such a field flip can be provided by a rotational shearing interferometer (Diner 1989, Shao 1989). In this approach, the flat end mirrors in the two arms of a laboratory Michelson interferometer are replaced by a pair of rooftop mirrors oriented so that they appear orthogonal when viewed in projection from the common output beam. Each individual rooftop mirror reverses only that component of the incident field which is perpendicular to the rooftop apex line (Fig. 4). With a pair of orthogonal rooftop mirrors behind a beamsplitter, both polarization components are then flipped relative to each other (Fig. 5). In addition to flipping the **E**-fields, the rooftop mirrors also shear the return beams symmetrically across the rooftop centerlines (Fig. 6), so that two input beams arriving at opposite corners of the input field yield two nulled and two bright (or constructive) outputs, all of which are spatially separated from the input beams.

However, one problem with the rotational shearing interferometer described (Fig. 7, left side) is that a significant asymmetry exists between the interferometer's two arms: light of a given polarization state (s- or p-plane polarization at the beamsplitter) undergoes 2 s-plane reflections at one of the rooftop mirrors, but 2 p-plane reflections at the other. Thus incident light in the two polarization states emerges with nonzero and opposite s-p phase delays. Luckily, it is possible to symmetrize the situation by inserting properly oriented 45° fold mirrors prior to the rooftops, as in Fig. 7, so that light in each arm of the modified interferometer sees 2 s-plane and 2 p-plane reflections, all at 45° angle of incidence (Shao 1991, Diner *et al.* 1991). This results in the overall optical layout shown in Fig. 8.

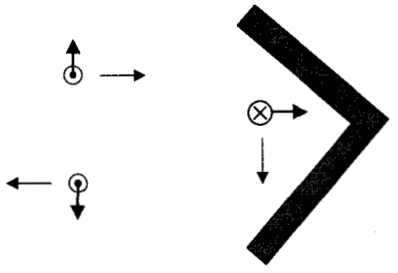

Figure 4. Side view of a rooftop (dihedral) mirror, illustrating the fact that only the component of the incident **E***-field which is normal to the rooftop apex emerges reversed in direction.*

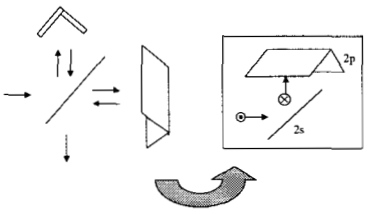

Figure 7. Diagram illustrating the extra fold mirror needed to symmetrize the reflections in the two arms of a rotational shearing interferometer.

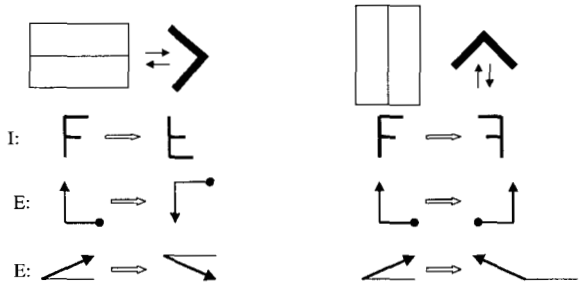

Figure 5. Illustration of the action of two orthogonal rooftop mirrors. I *refers to the image plane, and* E *to the* **E***-field. Both the image plane and the* **E***-field show a relative inversion.*

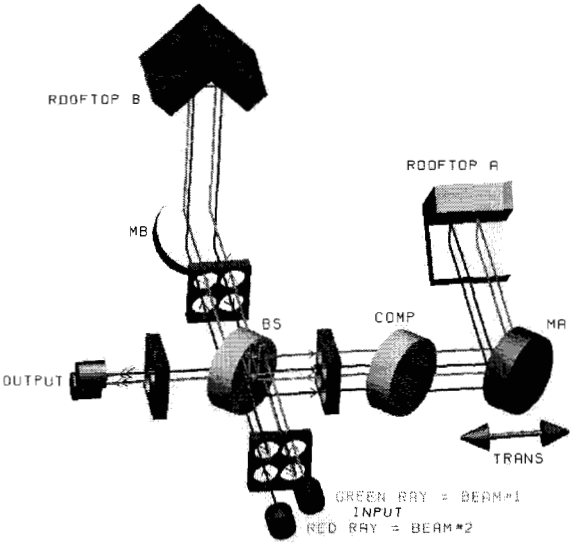

Figure 8. Optical layout of a symmetrized rooftop-based rotational shearing interferometer. The four aperture masks are guides for the eye.

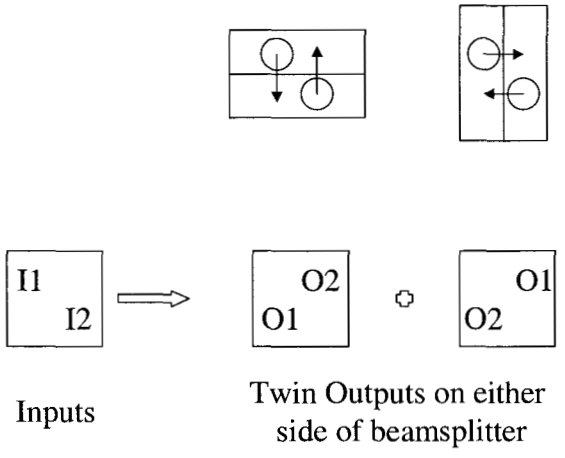

Figure 6. Illustration of the lateral beam shear obtained in a nulling beam combiner based on a pair of orthogonal rooftops. The two inputs yield four outputs, two of which are nulling outputs.

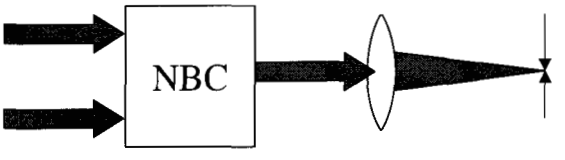

Figure 9. Diagram showing the use of a single-mode spatial filter to clean up the wavefront. NBC refers to the collimated nulling beam combiner.

4. SYMMETRY AND STABILITY REQUIREMENTS

The on-axis cancellation of stellar radiation requires a very symmetric and stable optical system. In particular, for a given polarization state, the two beam intensities, electric field rotation angles and phase delays must all be matched to $2\sqrt{N}$ (Serabyn, in prep.), where N, the null depth, is given by $N = I_{min}/I_{max}$, the ratio of the destructive minimum and constructive maximum transmissions. Thus for a net null depth of 10^{-6}, the allowable fractional intensity mismatch (the fractional deviation of either beam intensity from the mean), the relative rotation angle, and the phase difference must all be individually less than about 10^{-3} (the latter two in radians). Moreover, these conditions must also be met simultaneously for both polarizations, at every point across the aperture, and for all wavelengths in the band.

Satisfaction of the condition of simultaneous nulling across the full beam aperture necessitates an additional optical modification, as this condition effectively means translating the aforementioned phase matching requirement into a surface accuracy requirement. As a phase accuracy of 10^{-3} radians at a wavelength of 10 μm implies a surface accuracy of order 1 nm, it is clear that this goal cannot be met even with the finest optical surfaces available, and thus another approach is necessary. Indeed, if S is the beam Strehl ratio, attainable null depths would be limited to $\sim 1 - S$, or 10^{-2}. However, this limitation can be overcome (Fig. 9) by means of spatial filtering in the output focal plane (Shao 1991, Ollivier & Mariotti 1997), because the central value of the focal-plane point spread function is the Fourier transform of the *average* aperture-plane field. Thus the focused nuller output beam needs to be passed through a single-mode spatial filter, i.e., a single mode fiber at optical wavelengths, or a pinhole in the mid-infrared. This effectively limits operation to a single diffraction-limited mode of the telescope aperture, and so an analogy to single-dish, single-detector radio astronomy is not inappropriate.

5. EXPERIMENTAL RESULTS

A fiber-coupled rotational shearing interferometer of the type described (Fig. 8) has been built at the Jet Propulsion Laboratory (Serabyn *et al.* 1999, 2000) in order to evaluate the potential of the approach (Fig. 10). To date, the experiments have proven quite successful, verifying essentially all aspects of the fiber-coupled rotational shearing interferometer approach except for dual-polarization operation. Indeed, after many cycles of component and environmental improvements, null depths of 10^{-5} are now achieved regularly (Fig. 11) with a narrowband (0.5%) visible-wavelength laser diode source (Serabyn *et al.* 1999), and transient laser nulls as deep as 2×10^{-6} have been seen. In addition (Fig. 12), transient white light nulls of order 10^{-4} have been achieved for 10%

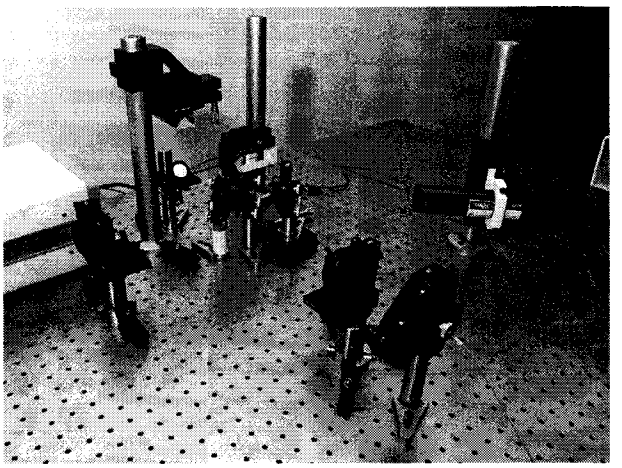

Figure 10. Experimental table-top fiber-coupled rotational shearing interferometer developed at JPL. The orientation is similar to Figure 8. The fiber input and collimating lens are at the lower right, the two rooftops toward the center and upper left, and the output lens toward the left.

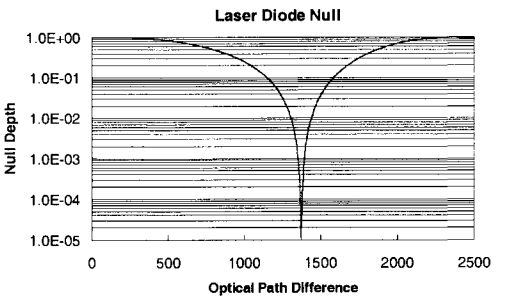

Figure 11. Experimental results from JPL's laboratory fiber-coupled nulling interferometer. An OPD scan through the position of the expected central null fringe shows a central null of 1×10^{-5}.

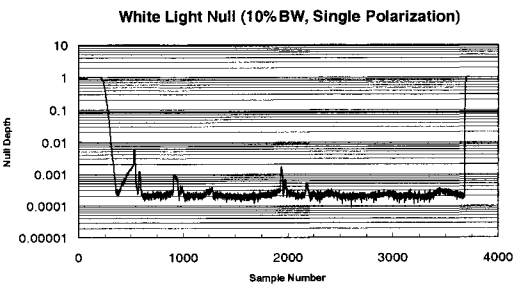

Figure 12. White light (10% bandwidth, single polarization) results from JPL's laboratory fiber-coupled nulling interferometer. The plot shows a time sequence of the nuller output at 10 Hz sampling. The OPD was under manual control. Near sample number 250, the nuller was taken from a state of constructive interference to the null position. Several additional manual retunings (brief upward spikes) are also evident. A best null of 1/11,000 is present, and short-term average nulls as deep as 1/5000 are seen.

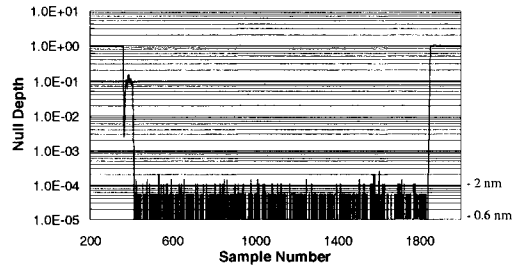

Figure 13. Stabilized laser null. The plot shows a time sequence of the nuller output at 50 Hz sampling. Near sample number 400, a pathlength-dither control loop was turned on, locking the OPD at the null position. Near sample number 1800, the phase of the loop was flipped by 180°, thereby locking onto a neighboring constructive interference peak.

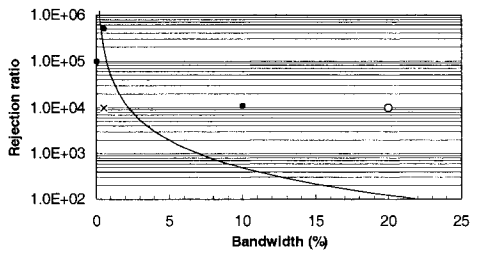

Figure 14. Current experimental status. Filled circles show the best transient nulls achieved to date, the cross shows the best stabilized null results, and the open circle shows the goal of the nulling experiment planned for the Space Interferometer Mission (SIM). The curve shows the best rejection achievable with a standard laboratory Michelson interferometer.

bandwidth, single-polarization, thermal (red) light (see also Serabyn *et al.* 2000). Finally, active stabilization of the laser null (Fig. 13) to a part in 10^4 has also been achieved (Serabyn *et al.* 1999), implying path length control of order 1 nm.

The current status of the experiments at JPL is summarized in Fig. 14. Note that the white light nulls achieved to date are far deeper than a standard Michelson interferometer can provide, thus verifying the achromatic nature of the nulling enabled by the field flip approach. Thus at this point, the major goals remaining for the complete validation of the nulling approach to planet detection are a broadening of the bandwidth over which deep nulls can be obtained, demonstration of dual polarization nulling, demonstration of equivalent nulling capabilities in the mid-infrared, and finally, definition of the overall multi-baseline interferometer configuration for envisioned space-based nulling missions such as ESA's Darwin and NASA's Terrestrial Planet Finder.

ACKNOWLEDGMENTS

The laboratory experiments described herein were carried out with the assistance of J. K. Wallace, G. J. Hardy, H.T. Nguyen and E.G.H. Schmidtlin. This research was carried out at the Jet Propulsion Laboratory, California Institute of Technology, under contract with the National Aeronautics and Space Administration.

REFERENCES

Angel, R. 1998, in "Exozodiacal Dust Workshop", NASA/CP 1998-10155, eds. D.E. Backman, L.J. Caroff, S.A. Sanford & D.H. Wooden, p. 209

Beichman, C.A., Woolf, N.J. & Lindensmith, C.A. 1999, Terrestrial Planet Finder, JPL publ. 99-3

Bracewell, R.N., 1978, Nature 274, 780

Bracewell, R.N., MacPhie, R.H., 1979, Icarus 38, 136

Diner, D.J. 1989, in *The Next Generation Space Telescope*, ed. P.Y. Bely, C.J. Burrows & G.D. Illingworth, p. 133

Diner, D.J., Tubbs, E.F., Gaiser, S.L., Korechoff, R.P., 1991, Jour. British Interplanetary Soc. 44, 505

Leger, A., Mariotti, J.M., Mennesson, B., Ollivier, M., Puget, J.L., Rouan, D., Schneider, J., 1996, Icarus, 123, 249

Ollivier, M., Mariotti, J.M., 1997, Applied Optics 36, 5340

Serabyn, E., Colavita, M.M., Beichman, C.A. 2000, in *Thermal Emission Spectroscopy of Dust, Disks, and Regoliths*, ed. M.L. Sitko, A.L. Sprague, D.K. Lynch, ASP Conf. Series Vol. 196, in press

Serabyn, E., Wallace, J.K., Nguyen, H.T., Schmidtlin, E.G.H., Hardy, G.J., 2000, in *Working on the Fringe: Optical and IR Interferometry from Ground and Space*, ed. S. Unwin, R. Stachnik, ASP Conf. Ser. Vol. 194, in press

Serabyn, E., Wallace, J.K., Hardy, G.J., Schmidtlin, E.G.H., Nguyen, H.T., 1999, Applied Optics 38, 7128

Shao, M. 1989, in *The Next Generation Space Telescope*, ed. P.Y. Bely, C.J. Burrows & G.D. Illingworth, p. 160

Shao, M. 1991, in *Space Astronomical Telescopes and Instrumentation*, ed. P.Y. Bely & J.B. Breckinridge, Proc. SPIE, 1491, 347

Shao, M., Colavita, M.M., 1992, Ann. Rev. Astron. Astrophys. 30, 457

Traub, W.A., Carleton, N.P., & Angel, J.R.P. 1996, in *Science with the VLT Interferometer*, ed. F. Paresce, Springer, p. 80

Woolf, N., Angel, J.R., 1998, Ann. Rev. Astron. Astrophys. 36, 507